PLOS ONE

RESEARCH ARTICLE

Bend-resistant leaky multi-trench fiber with large mode area and single-mode operation

Shaoshuo Ma[1], Tigang Ning[1], Li Pei[1]*, Jing Li[1], Jingjing Zheng[1], Xueqing He[1], Xiaodong Wen[2]

1 Key Lab of All Optical Network & Advanced Telecommunication Network of EMC, Institute of Lightwave Technology, Beijing Jiaotong University, Beijing, China, **2** College of Physics and Engineering, Qufu Normal University, Qufu, China

* lipei@bjtu.edu.cn

Citation: Ma S, Ning T, Pei L, Li J, Zheng J, He X, et al. (2018) Bend-resistant leaky multi-trench fiber with large mode area and single-mode operation. PLoS ONE 13(8): e0203047. https://doi.org/10.1371/journal.pone.0203047

Editor: Silvia Vignolini, University of Cambridge, UNITED KINGDOM

Received: November 24, 2017

Accepted: August 14, 2018

Published: August 30, 2018

Data Availability Statement: All relevant data are within the paper.

Funding: This work was supported by the National Natural Science Foundation of China (NSFC-61525501), http://www.nsfc.gov.cn/. The funders had no role in study design, data collection and analysis, decision to publish, or preparation of the manuscript.

Competing interests: The authors have declared that no competing interests exist.

Abstract

A novel structure of modified multi-trench fiber (MTF) with characteristics of bend-resistance and large mode-area is proposed. In this structure, each low refractive-index trench of traditional MTF is broken by two gaps up and down. Numerical investigations show that the mode field area of 840 μm^2 can be achieved with effective single-mode (SM) operation when the bending radius is 15 cm. Moreover, the high order mode (HOM) suppression of the proposed design is better than that of standard MTF. The SM operation property can be enhanced with the decreases of bending radius. The proposed design shows great potential in high power fiber lasers with compact structure.

Introduction

Over the last decades, high power fiber lasers have developed rapidly due to their beam quality, heat dissipation, brightness, operating costs and efficiency [1–3]. However, with the further increase of output power, the nonlinear effect of fiber becomes the most important challenge. To eliminate the challenges induced by high power output, large mode area (LMA) fibers have become the preferred choice.

A large number of transverse modes always lead to the mode competition and instability of output [4, 5]. It is important for high power fiber lasers to achieve LMA and effective single-mode (SM) operation simultaneously. A series of LMA fibers have been proposed to achieve effective SM operation, such as double-clad fibers [6], low numerical aperture (NA) step-index fibers [7], chirally-coupled-core (CCC) fibers [8], photonic crystal fibers (PCF) [9], segmented cladding fibers (SCF) [10,11], gain-guided and index anti-guided (GG+IAG) optical fibers [12], microstructured fibers [13, 14], multilayer cladding fibers [15–17] and multi-trench fibers (MTFs) [18–20]. However, the application limits of these fibers are the complex and expensive fabrication and detrimental bending effects.

Rod MTFs can achieve large mode area and excellent high-order modes (HOMs) suppression capability [19]. However, when MTF is bent, the mode region must be less than 800 μm^2 in order to maintain the HOMs suppression capability. The mode area is about 410 μm^2 with

30 μm core diameter when bending radius is 20 cm. Sun et al. broke gaps on two outer trenches to improve the bending performance [21,22].

In this paper, we demonstrate that all trenches broken MTF can improve the SM operation outstandingly. The gap width can be adjusted to control the leakage losses of the fiber. The loss ratio between lowest-HOM and fundamental mode (FM) is more than 300 with the mode area of 840 μm^2 under bending radius of 15 cm. The propagation characteristics with different fiber parameters are also discussed in detail.

Optical fiber structure and theoretical model

The proposed modified MTF structure is shown in Fig 1. The leaky-MTF can be fabricated by carving grooves in MTF and inserting rods into these grooves [21, 22]. The gray region represents the low refractive-index (RI) of $n_2 = 1.444$ at the wavelength of 1064 nm. The yellow region represents the high RI (n_1). The notations are also shown in Fig 1, where a stands for core radius. t_1, t_2 and t_3 are the thickness of low RI trenches, respectively. d_1 and d_2 are the thickness of high RI rings, respectively. $\Delta n = n_1 — n_2$ is the RI difference between the core and

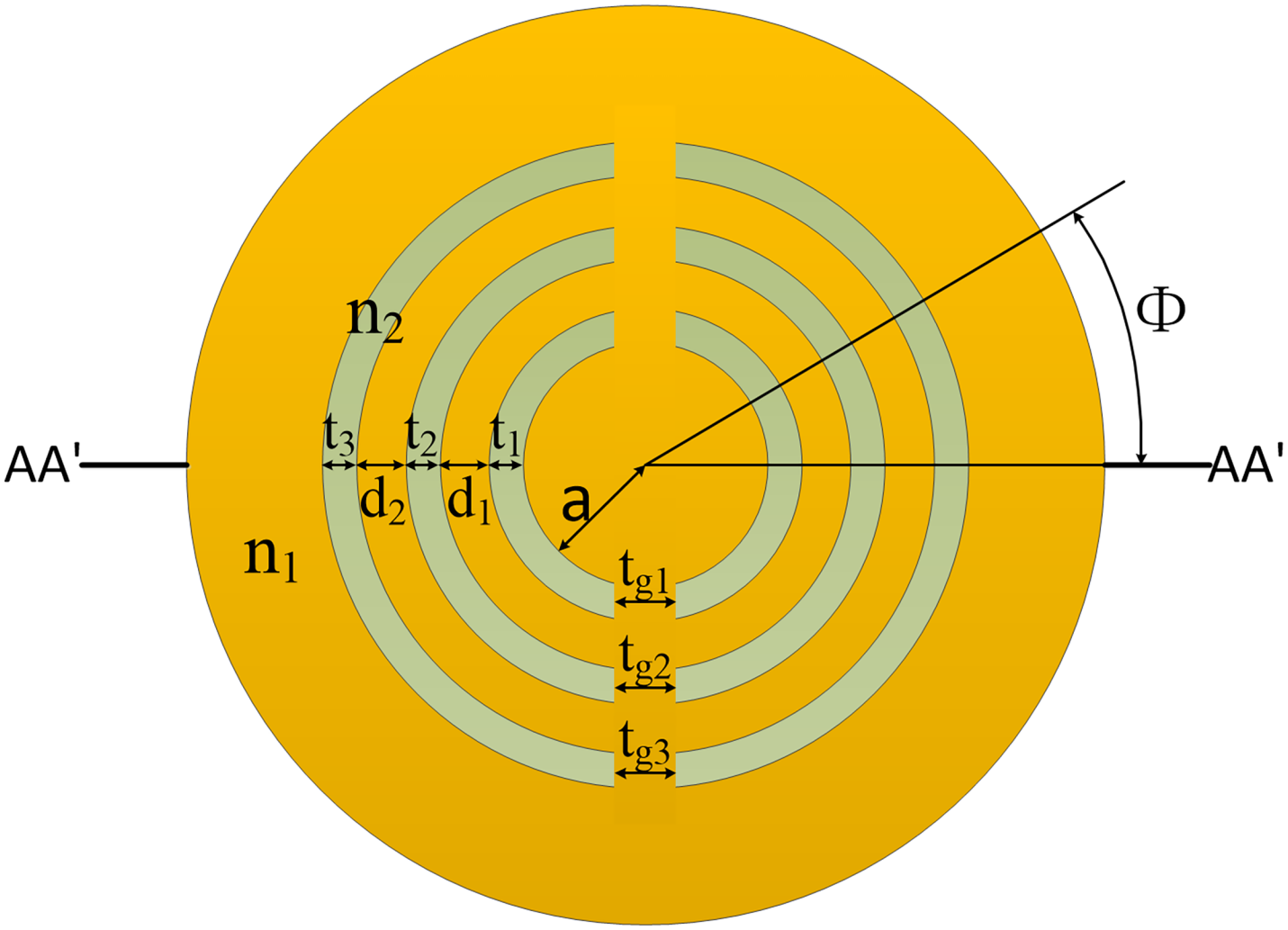

Fig 1. Cross section and notations of the proposed leaky-MTF with leakage gaps.

https://doi.org/10.1371/journal.pone.0203047.g001

the low RI trenches. t_{g1}, t_{g2} and t_{g3} are the gap width, respectively. Φ is the bending angle between the actual bending orientation and the reference bending orientation (*AA*'). It should be noted that, when we mention *t*, it represents all the low RI trenches (t_1, t_2 and t_3). For example, when t = 3 μm, it represents $t_1 = t_2 = t_3$ = 3 μm. For *t* ranges from 3–9 μm, it denotes t_1, t_2 and t_3 range from 3–9 μm simultaneously. Similarily, *d* represents d_1 and d_2; t_{gap} represents t_{g1}, t_{g2} and t_{g3}.

The finite element method (FEM) is used in complex fiber structure analysis due to its high calculation precision. It is the most commonly used method in microstructure optical fiber simulation. The numerical simulations are calculated by using COMSOL Multiphysics software based on FEM, together with anisotropic perfectly matched layers (PMLs). For the proposed theoretical analysis of leaky-MTF, a 20-μm-thick circular PML is set outside the fiber cladding. Bending has an effect on the RI distribution of silica optical fiber. The bent fiber can be equivalent to a straight fiber through a proper mathematical transformation. After being modified with additional stress perturbations, the bent fiber RI distribution $n'(x,y)$ can be expressed as [23,24]:

$$\mathrm{n}'(\mathrm{x},\mathrm{y}) = n(x,y) * (1 + \frac{\overrightarrow{x}\cos\Phi + \overrightarrow{y}\sin\Phi}{\rho * R}) \tag{1}$$

where $n(x,y)$ is the initial RI distribution of straight fiber, *R* is bending radius, Φ is the bending orientation angle (as shown in Fig 1) and ρ (here fixed to 1.25) is correction coefficient taking account of the stress factor.

Bending loss and mode area A_{eff} can be calculated by the following equations [25, 26]:

$$Loss = \frac{40\pi}{ln(10)\lambda} Im(n_{eff}) \tag{2}$$

$$A_{eff} = \frac{(\iint |E^2| dxdy)^2}{\iint |E|^4 dxdy} \tag{3}$$

Where n_{eff} is the effective RI of modes, *E* is the electric field inside the fiber and λ is the operation wavelength, which is set as 1064 nm in this paper. Defaultly, the reference bending direction is *AA*' (Φ = 0˚), if not specially mention. In practical applications, FM loss less than 0.1 dB/m and HOMs loss more than 1 dB/m is considered as the basic condition of effective SM operation [27].

The loss ratio (LR) means ratio between lowest-HOM and FM in fiber, which is defined as

$$LR = \frac{Loss(lowest - HOM)}{Loss(FM)} \tag{4}$$

Where *Loss (lowest-HOM)* is the loss of lowest-HOM and *Loss (FM)* is the loss of fundamental mode. In this paper, $Loss(LP_{01})$ refers to the loss of LP_{01} mode, $Loss(LP_{11v})$ refers to the loss of LP_{11v} mode, $Loss(LP_{11h})$ refers to the loss of LP_{11h} mode.

Method verification

In order to confirm the accuracy of the simulation method and contrast the difference with our design, we simulate the standard MTF firstly. The standard MTF with structural parameters a = 15 μm, t = 2 μm, d = 8 μm and Δn = 0.005 as that in [18] is simulated at wavelength of 1064 nm. Fig 2(A) shows the numerically simulated losses of the FM and HOMs of standard MTF as a function of bending radius. Fig 2(B) shows the simulated A_{eff} of the FM. The inset pictures show the simulated normalized electric field of LP_{01}, LP_{11v}, LP_{11h} and LP_{11like} mode at

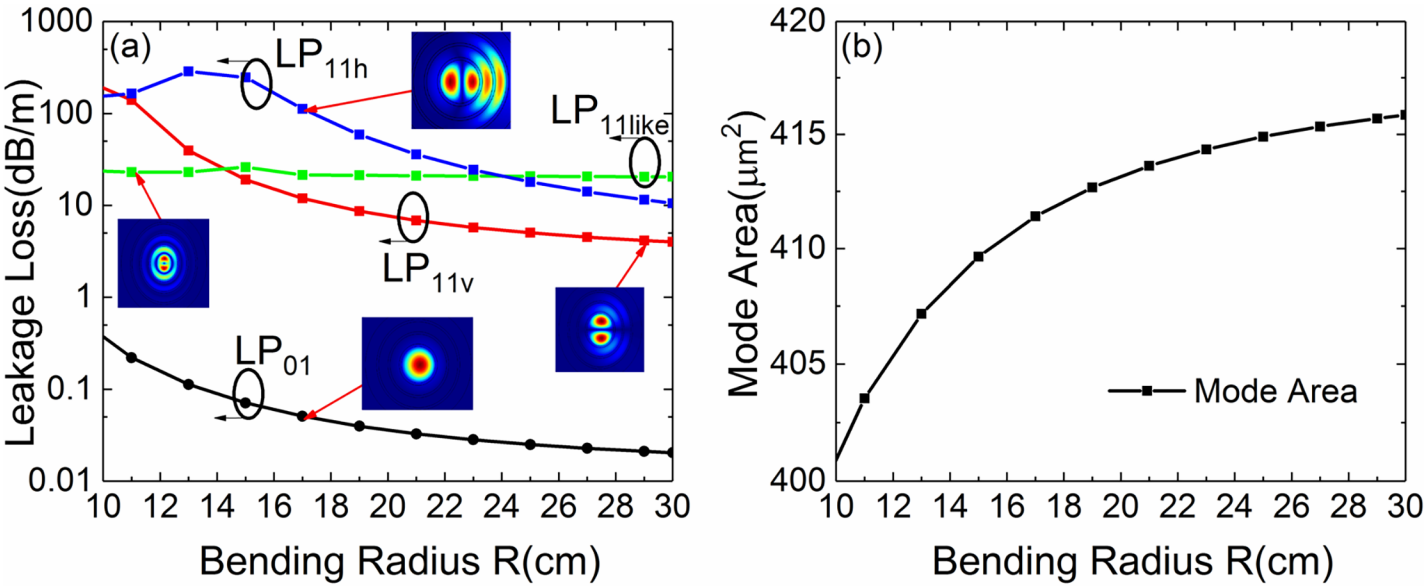

Fig 2. Fiber performance with different bending radius. (a) Simulated losses of the FM and HOMs of the standard MTF with a = 15 μm, t = 2 μm, d = 8 μm and Δn = 0.005 for different bend radii. Inset pictures show the computed normalized electric field of the FM and HOMs at a bend radius of 17 cm, 29 cm, 21 cm and 11 cm, respectively. (b) The A_{eff} for the FM at different bend radii.

https://doi.org/10.1371/journal.pone.0203047.g002

a bending radius of 17 cm, 29 cm, 21 cm and 11 cm, respectively. When bending radius ranges from 10 cm to 14 cm, the lowest-HOM is LP_{11like} mode. When bending radius ranges from 14 cm to 30 cm, the lowest-HOM is LP_{11} mode. The A_{eff} remains larger than 400 μm^2 when bending radius ranges from 10–30 cm. The computed data are similar to the results given in Ref.18. Therefore, the accuracy of the simulation method in this paper is reliable.

It can be seen from Fig 2(A) that, LP_{11v} and LP_{11h} mode are separated because of the birefringence caused by bending. LP_{11h} mode suffers more leakage loss than LP_{11v} mode. We propose leaky-MTF by breaking two gaps up and down on each low RI trench, as shown in Fig 1. The effects of gaps are shown in the following chapters.

Numerical simulations

Effects of gaps

Fig 3(A) shows the leakage loss of LP_{01}, LP_{11v}, LP_{11h} and lowest-HOMs for different gap width. The other fiber parameters are the same as Fig 2. The LR is also plotted in Fig 3(A) (right axis). The A_{eff} is shown in Fig 3(B). The losses of LP_{01} and LP_{11v} mode increase when t_{gap} enlarges. The loss of LP_{11h} mode remains stable when t_{gap} changes from 0–6 μm but increases when t_{gap} is larger than 6 μm. To illustrate this case, the contour line graphs of the mode field distribution of three modes with t_{gap} = 0 μm, 4 μm, 6 μm, 7 μm and 8 μm are shown in Fig 4. LP_{11h} mode remains stable when t_{gap} changes from 0–6 μm because the mode distribution is far from gap. At t_{gap} = 4 μm, the mode leakage of LP_{11v} mode is equal to LP_{11h} mode ($Loss(LP_{11v})$ = $Loss(LP_{11h})$). It is the first peak value for lowest-HOMs. When t_{gap} is larger than 6 μm, the mode distribution is close to gap and the leakage of LP_{11h} mode increase. However, At t_{gap} = 7 μm, $Loss(LP_{11h})$ has the peak value because the leakage and resonance reach the largest. It is the second peak value for lowest-HOMs. Corresponding with lowest-HOMs, it has optimum values at t_{gap} = 4 μm and 7 μm.

For standard MTF (t_{gap} = 0), the loss of LP_{01}, LP_{11v} and LP_{11h} mode is 0.004, 0.56 and 3.8 dB/m, respectively. For t_{gap} = 4 μm, the loss of LP_{01}, LP_{11v} and LP_{11h} mode is 0.01, 3.6 and 3.9

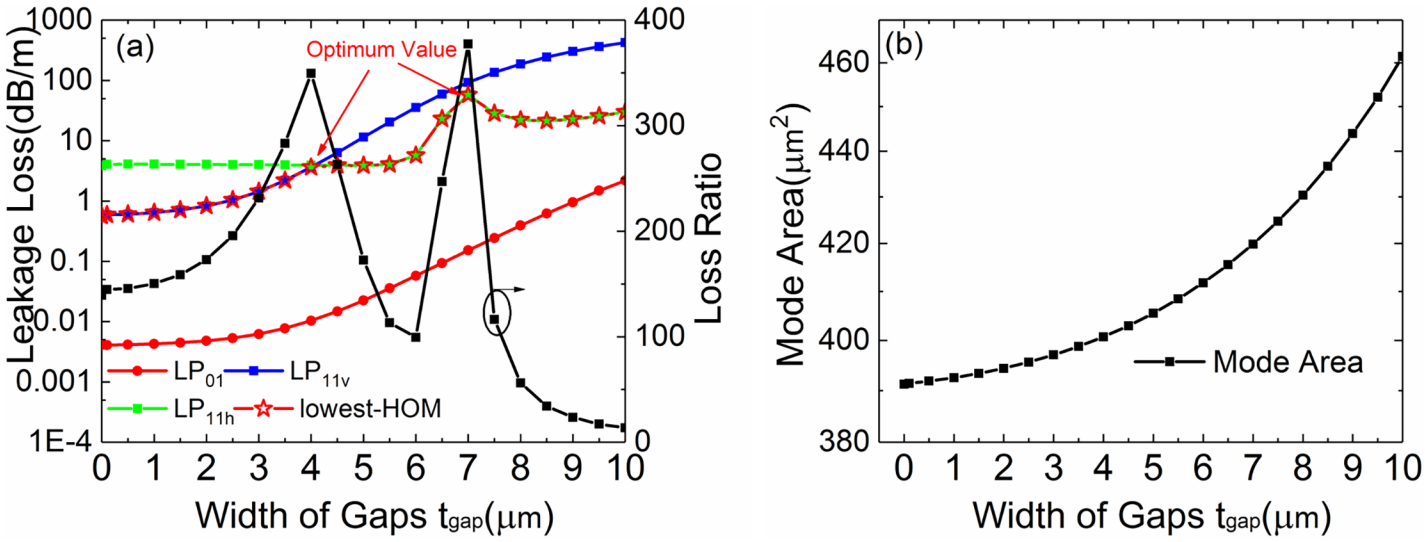

Fig 3. Fiber performance with different width of gaps. (a) Simulated losses of the FM and HOMs and LR of the leaky-MTF with a = 15 μm, t = 2 μm, d = 8 μm and Δn = 0.005 for different bend radii. (b) The A_{eff} for the FM at different bend radii.

https://doi.org/10.1371/journal.pone.0203047.g003

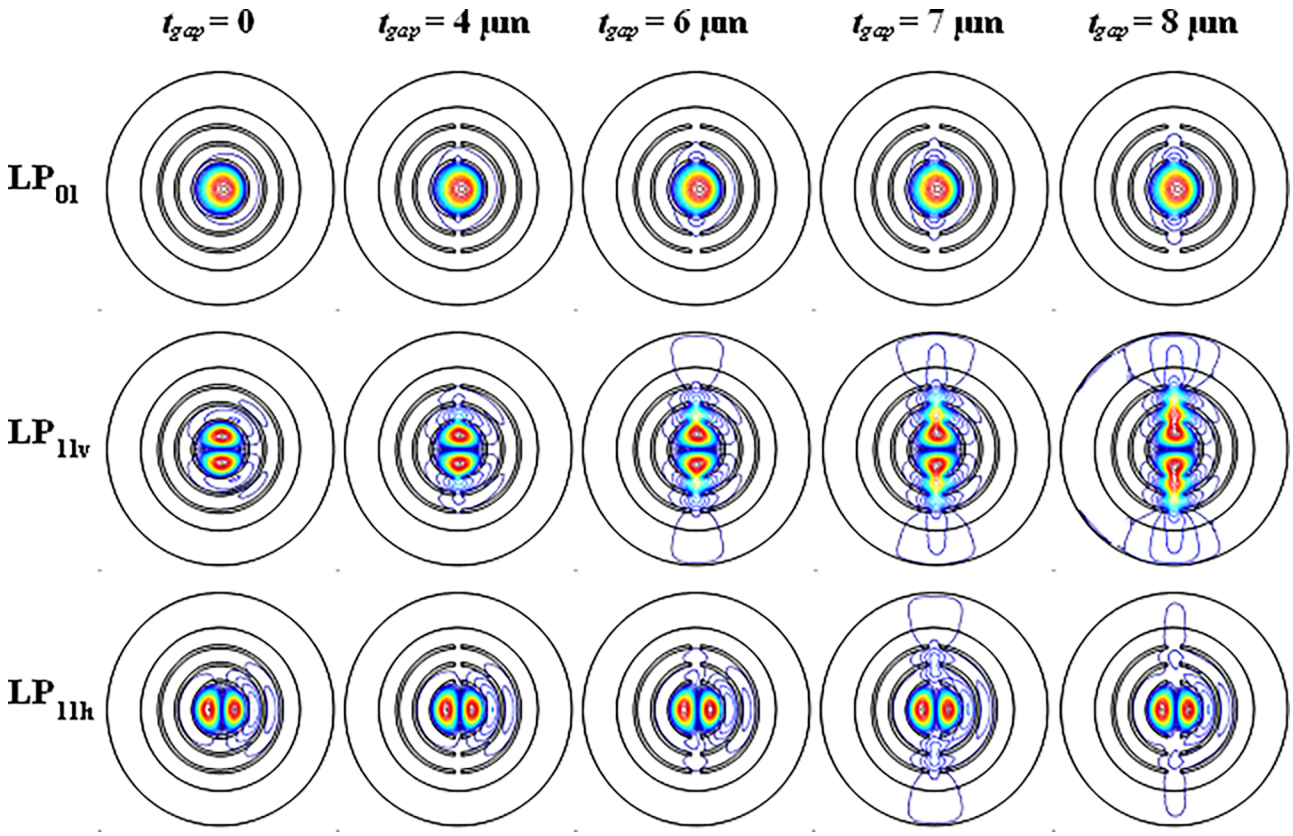

Fig 4. Contour line graphs of the mode field distribution of LP_{01}, LP_{11v} and LP_{11h} mode of the leaky-MTF with t_{gap} = 0, 4 μm, 6 μm, 7 μm and 8 μm.

https://doi.org/10.1371/journal.pone.0203047.g004

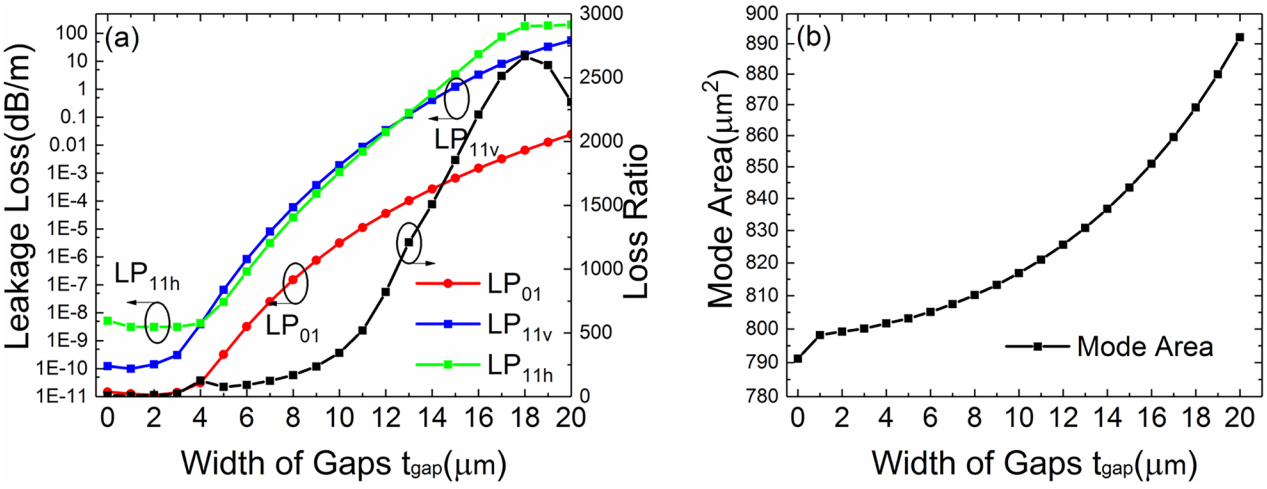

Fig 5. Fiber performance with different width of gaps. (a) Simulated losses of the FM and HOMs and LR of the leaky-MTF with a = 25 μm, t = 6 μm, d = 10 μm, R = 15 cm and Δn = 0.007 for different gap width. (b) The A_{eff} for the FM at different gap width.

https://doi.org/10.1371/journal.pone.0203047.g005

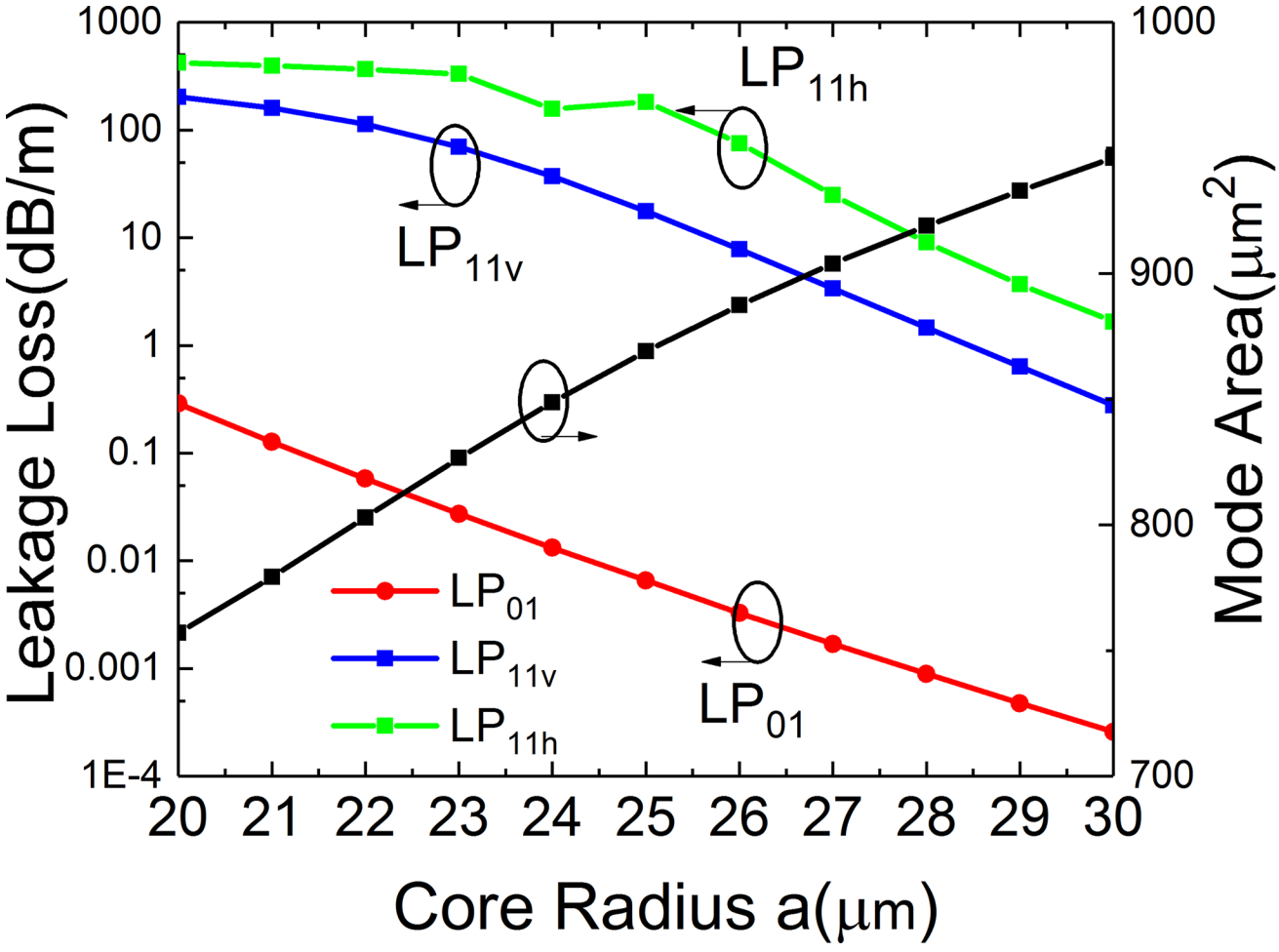

Fig 6. Simulated losses of the FM and HOMs and mode area of FM of the leaky-MTF with t_{gap} = 18 μm, t = 6 μm, d = 10 μm, R = 15 cm and Δn = 0.007 for different core radius.

https://doi.org/10.1371/journal.pone.0203047.g006

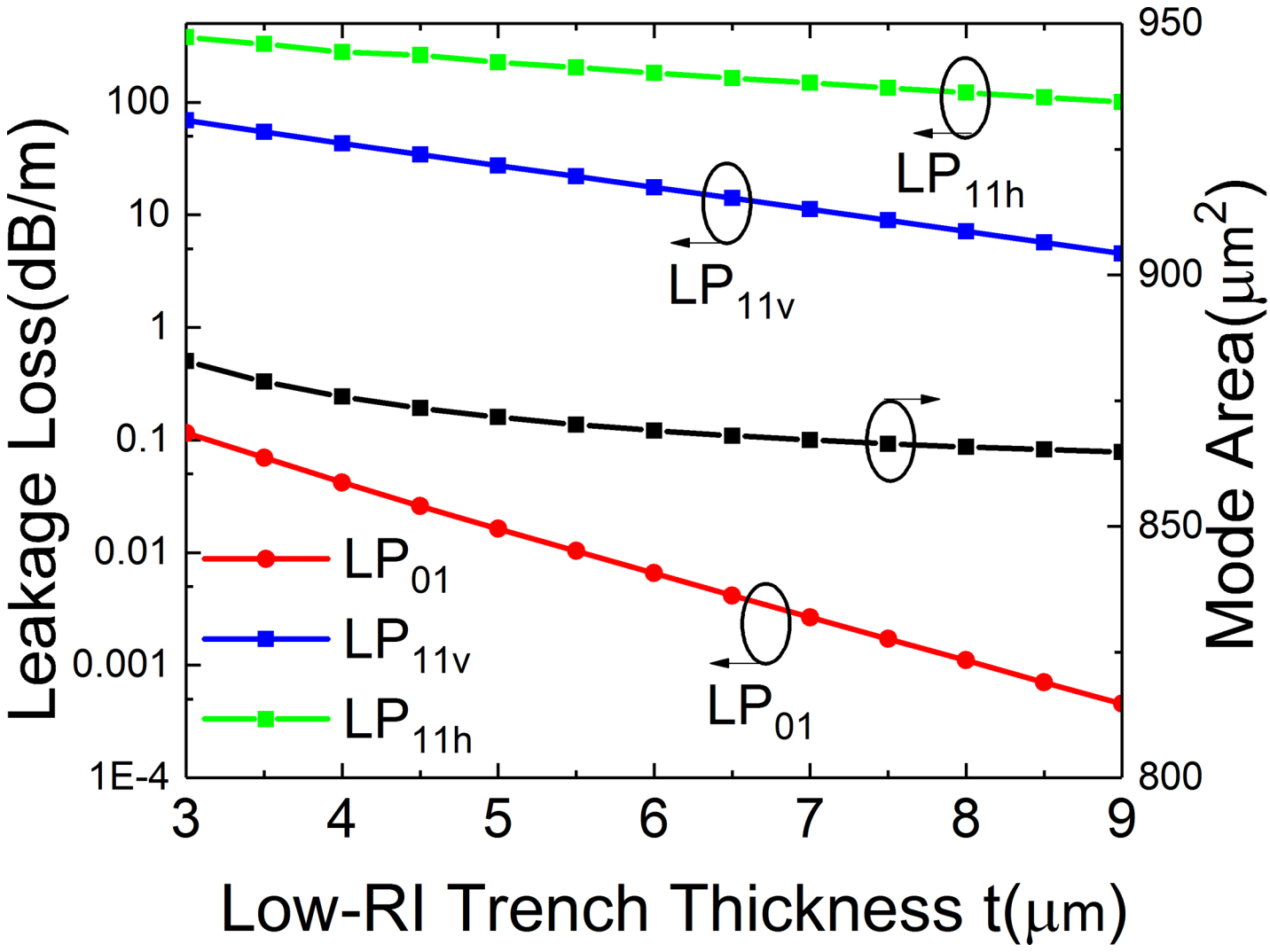

Fig 7. Simulated losses of the FM and HOMs and mode area of FM of the leaky-MTF with a = 25 μm, t_{gap} = 18 μm, d = 10 μm, R = 15 cm and Δn = 0.007 for different thickness of low RI trenches.

https://doi.org/10.1371/journal.pone.0203047.g007

dB/m, respectively. The LR increases by 150% from 139 to 350. For t_{gap} = 7 μm, the loss of LP_{01}, LP_{11v} and LP_{11h} mode is 0.15, 92 and 57 dB/m, respectively. The LR increases by 170% from 139 to 377. The introduction of gaps has an excellent improvement for SM operation. As shown in Fig 3, to achieve a high differential loss factor, a proper gap width is necessary. As the t_{gap} increases, the A_{eff} increases from 390 μm^2 to 460 μm^2.

In order to further enlarge the effective mode area, we choose the parameters of fiber as a = 25 μm, t = 6 μm, d = 10 μm, t_{gap} = 18 μm, Δn = 0.007 and R = 15 cm. The effects of various parameters of the structure are studied and summarized in Figs 5–17. Fig 5(A) shows the effect of the gap width on the loss of LP_{01}, LP_{11v} and LP_{11h} modes and LR. Fig 5(B) shows the effective mode are of FM. The variation trend of loss curves and LR curve are similar to Fig 3. The loss of LP_{01} and LP_{11v} mode increase with the increase of gaps. The loss of LP_{11h} mode keeps stable at first, and then increases. It can be seen from Fig 5(A) that, the LR has two peak values at $t_{gap} \approx 4$ μm and $t_{gap} \approx 18$ μm. For standard MTF (t_{gap} = 0), the loss of LP_{01}, LP_{11v} and LP_{11h} mode are 1.5×10^{-11}, 1.2×10^{-10} and 5×10^{-9} dB/m, respectively. The LR is 8.4 and the mode area

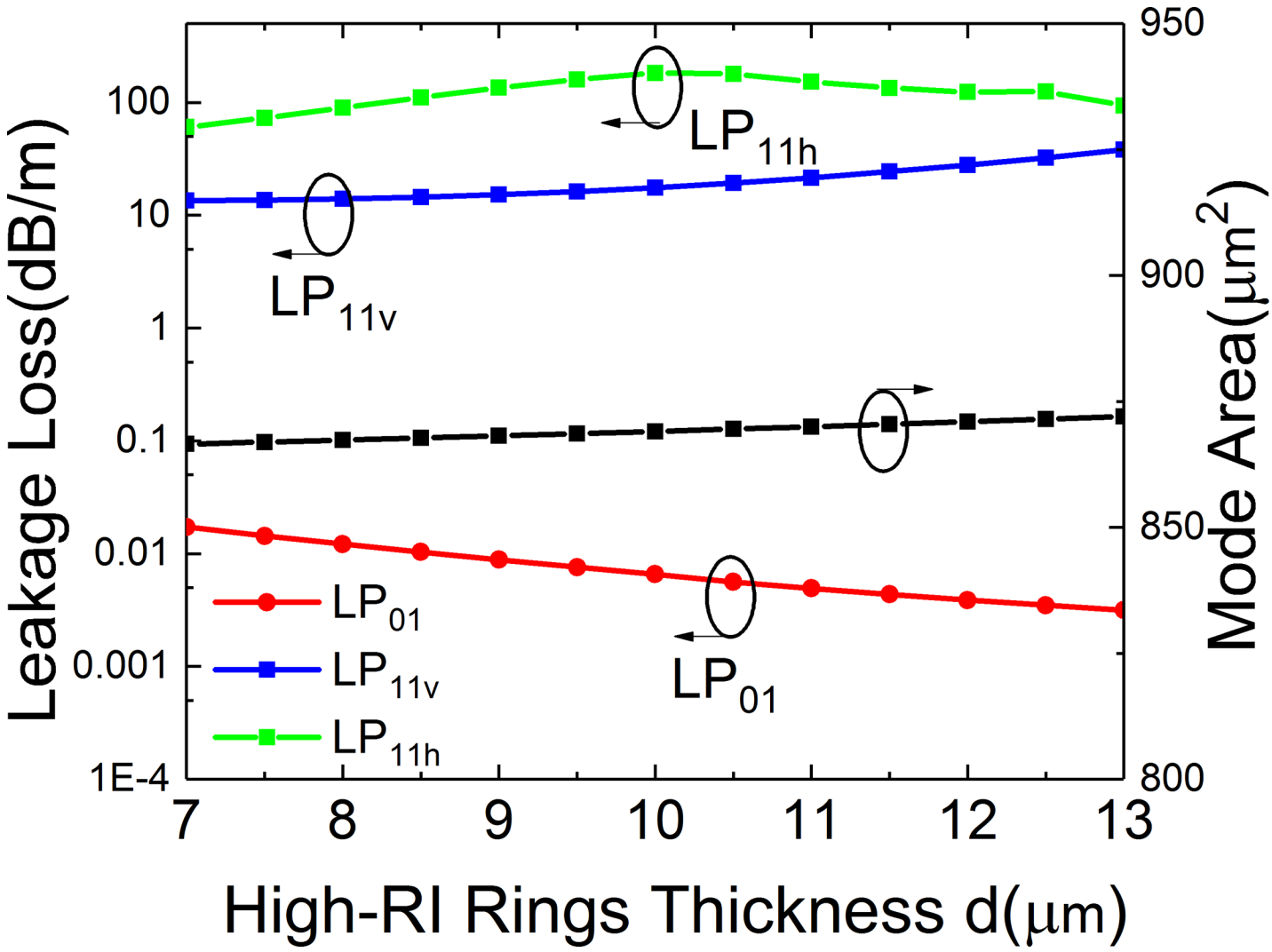

Fig 8. Simulated losses of the FM and HOMs and mode area of FM of the leaky-MTF with a = 25 μm, t = 6 μm, t_{gap} = 18 μm, R = 15 cm and Δn = 0.007 for different thickness of high RI rings.

https://doi.org/10.1371/journal.pone.0203047.g008

of FM is 791 μm^2. At t_{gap} = 4 μm, the loss of LP_{01}, LP_{11v} and LP_{11h} mode are 3×10^{-11}, 3.9×10^{-9} and 4.2×10^{-9} dB/m, respectively. The LR is 126 which arise by 1400% and the mode area of FM is 801 μm^2. At t_{gap} = 18 μm, the loss of LP_{01}, LP_{11v} and LP_{11h} mode are 0.006, 17 and 182 dB/m, respectively. The LR is 2667 which arises by 31600% theoretically and the mode area of FM is 869 μm^2.

It is clear that, gap can enlarge the core modes' leakage losses thus it allows short fiber length to trip off HOMs. Meanwhile, LR can be tuned by adjusting to the gap width. By considering the largest loss of LP_{11} mode and LR, we choose t_{gap} = 18 μm.

Effects of core radius

Fig 6 shows the variation of bending losses of the first three modes of fiber (LP_{01}, LP_{11v} and LP_{11h}) and A_{eff} of FM on core radius (a) of the proposed structure. When core radius increases, the losses of LP_{01}, LP_{11v} and LP_{11h} mode decrease, while A_{eff} increases. By considering the trade-off between bending loss and mode area, we choose a = 25 μm to achieve both LMA and

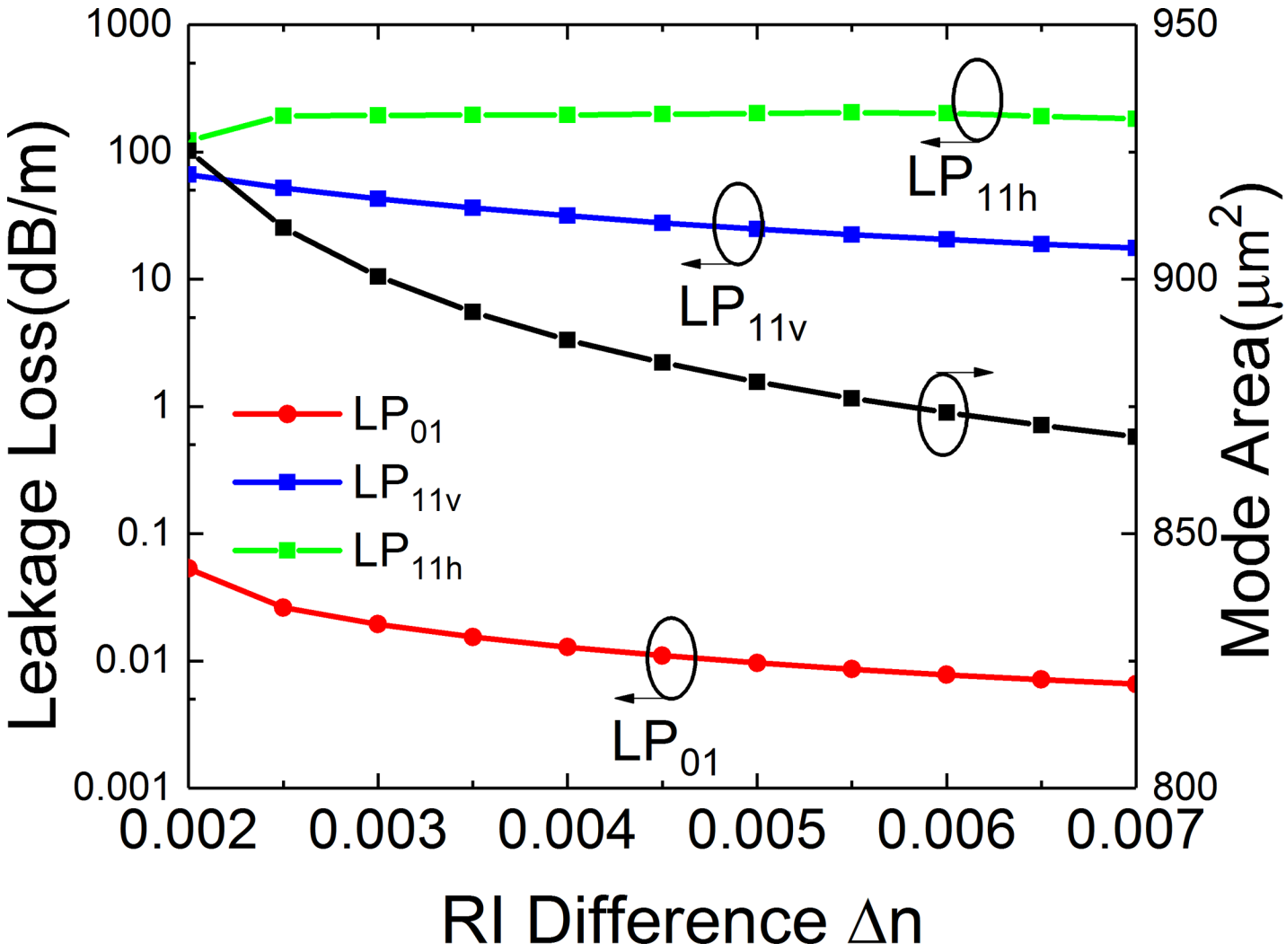

Fig 9. Simulated losses of the FM and HOMs and mode area of FM of the leaky-MTF with a = 25 μm, t_{gap} = 18 μm, t = 6 μm, d = 10 μm and R = 15 cm for different RI difference.

https://doi.org/10.1371/journal.pone.0203047.g009

effective SM operation. In this case, *Loss* (LP_{01}) < 0.01 dB/m and *Loss* ($LP11$) > 0.01 dB/m. Meanwhile, the A_{eff} = 869 μm^2.

Effects of low RI trenches

Fig 7 shows the effect of low RI trench thickness (t) on SM operation and A_{eff} of FM of the structure. It can be observed that the losses of LP_{11v} and LP_{11h} mode decrease slowly when t increases and the LP_{01} mode decreases sharply. The A_{eff} of FM also decreases when t increases. When t is in the range from 3.5 to 9 μm, the highest bending loss of LP_{01} mode is lower than 0.1 dB/m and the lowest bending loss for LP_{11} mode is higher than 4 dB/m, which is considered viable for SM operation. Meanwhile, the A_{eff} is larger than 850 μm^2.

Effects of high RI rings

Fig 8 illustrates the loss of LP_{01}, LP_{11v} and LP_{11h} and A_{eff} of FM under different d. It can be observed that the bending loss of LP_{01} mode decreases when d increases. The loss of LP_{11v}

mode and A_{eff} of FM have a slight increase when d increases. When d is in the range from 7 to 13 μm, the highest loss of LP_{01} mode is lower than 0.02 dB/m and the lowest loss of LP_{11} mode is large than 13 dB/m. Meanwhile, the A_{eff} ranges from 866 to 972 μm^2.

Effects of RI difference

The effects of the RI difference (Δn) are shown in Fig 9. The structural parameters are a = 25 μm, t_{gap} = 18 μm, t = 6 μm, d = 10 μm and R = 15 cm. Fig 9 illustrates leakage losses of LP_{01}, LP_{11v} and LP_{11h} mode and A_{eff} of FM. From Fig 9, it can be seen that Δn has a slight effect on LP_{01}, LP_{11v} and LP_{11h} mode and a serious effect on A_{eff} of FM. When Δn is in the range from 0.2 to 0.7, the highest loss of LP_{01} mode is lower than 0.06 dB/m and the lowest bending loss for LP_{11} mode is higher than 17 dB/m. It is considered that the bending loss conforms effective SM operation. The A_{eff} decreases from 925 to 869 μm^2.

Effects of wavelength

The effect of the wavelength (λ) have been investigated and presented in Fig 10. The A_{eff} of FM and bending losses of LP_{01} and LP_{11v} modes increase with the increases of λ. When λ is in the

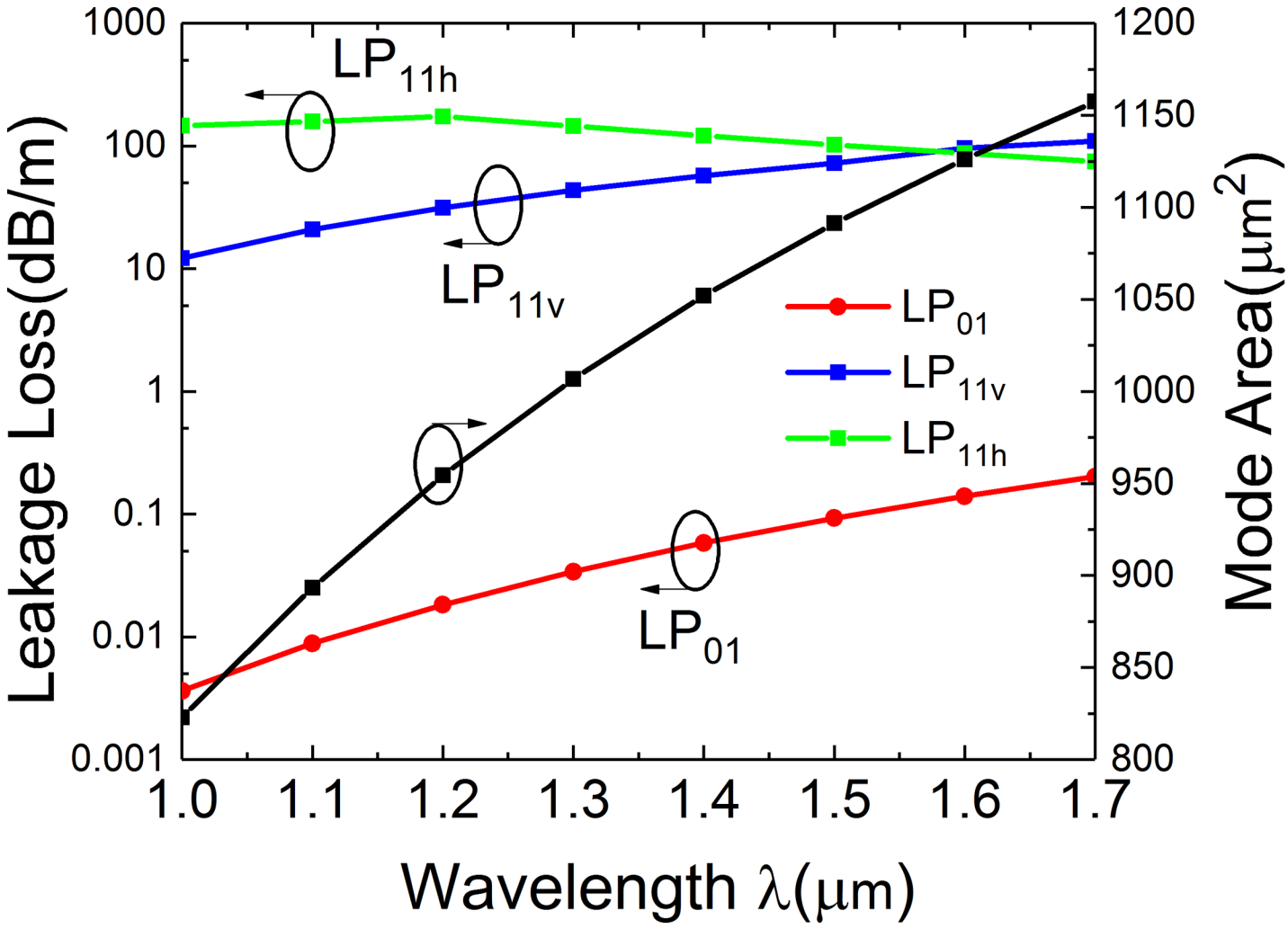

Fig 10. Simulated losses of the FM and HOMs and mode area of FM of the leaky-MTF with a = 25 μm, t_{gap} = 18 μm, t = 6 μm, d = 10 μm, R = 15 cm and Δn = 0.007 for different wavelength.

https://doi.org/10.1371/journal.pone.0203047.g010

range from 1 to 1.7 μm, the highest loss of LP_{01} mode is lower than 0.2 dB/m and the lowest bending loss of LP_{11} mode is higher than 12 dB/m. The A_{eff} of FM increases from 822 to 1157 μm^2. The fiber can achieve effective SM operation and LMA in a wide transmission bandwidth from 1 μm to 1.7 μm.

Effects of bending

The effects of bending are shown in Figs 11–13. Fig 11 illustrates the leakage losses of LP_{01}, LP_{11v} and LP_{11h} and mode area of FM at varying bending radius. The structural parameters are a = 25 μm, t = 6 μm, d = 10 μm, t_{gap} = 18 μm, Δn = 0.007 and $\Phi = 0^{\circ}$. When the bending radius ranges from 10 cm to 80 cm, the loss of LP_{01} is less than 0.05 dB/m and the loss of LP_{11} is larger than 5 dB/m. The A_{eff} ranges from 700 to 1130 μm^2.

Fig 12 shows the contour line graphs of the mode field distributions of LP_{01}, LP_{11v} and LP_{11h} modes of the leaky-MTF with R = 80 cm, 15 cm and 5 cm. *Loss (LP_{11h})* increases when R rangs from 80 cm to 5 cm. However, when the bending radius decreases, the losses of LP_{01} and LP_{11v} mode decrease. When R = 80 cm, the LP_{01} mode leaks from the gaps. When R = 5 cm,

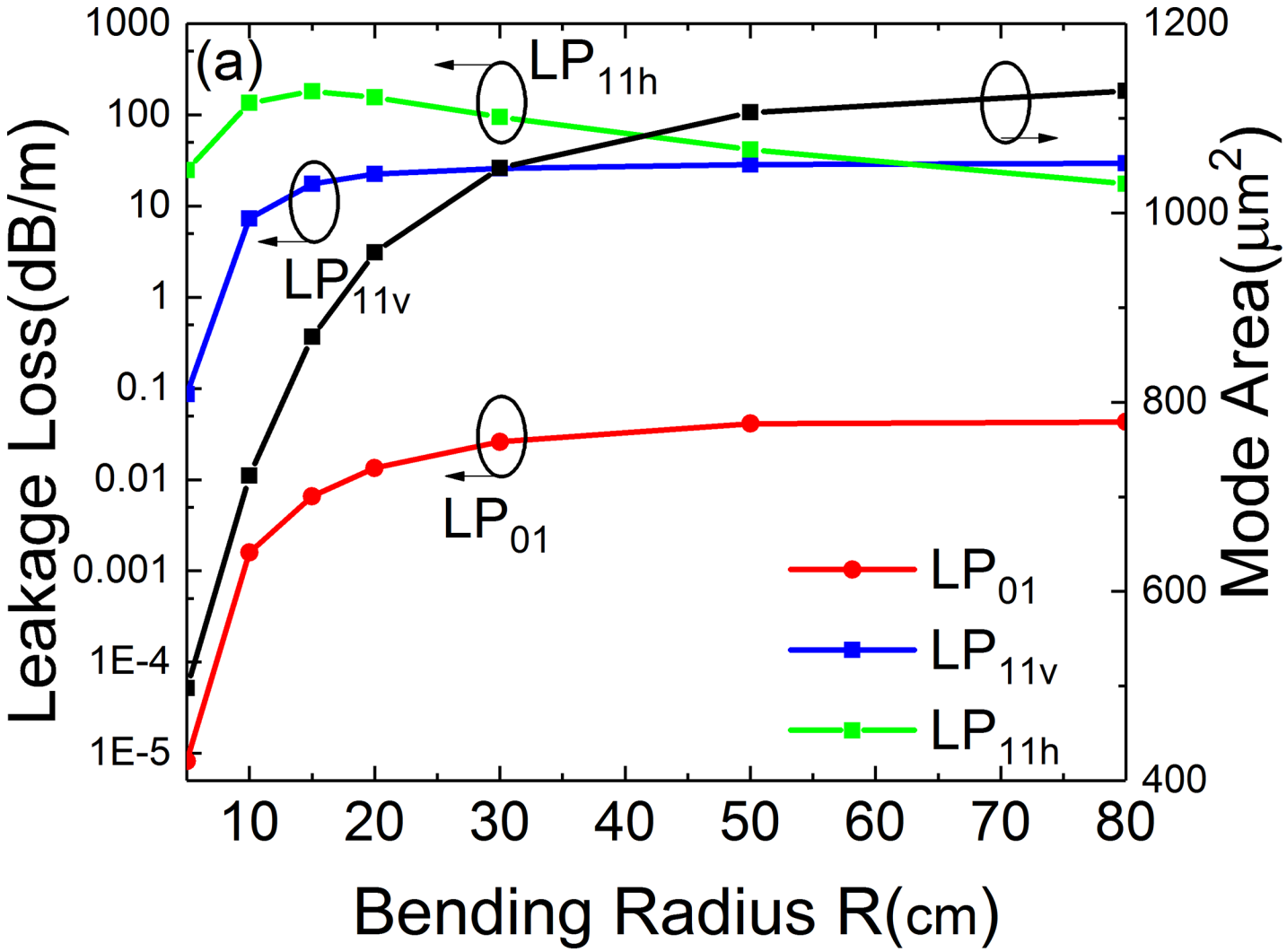

Fig 11. Simulated losses of the FM and HOMs and mode area of FM of the leaky-MTF with a = 25 μm, t = 6 μm, d = 10 μm, t_{gap} = 18 μm, Δn = 0.007 and $\Phi = 0^{\circ}$ for different bending radius.

https://doi.org/10.1371/journal.pone.0203047.g011

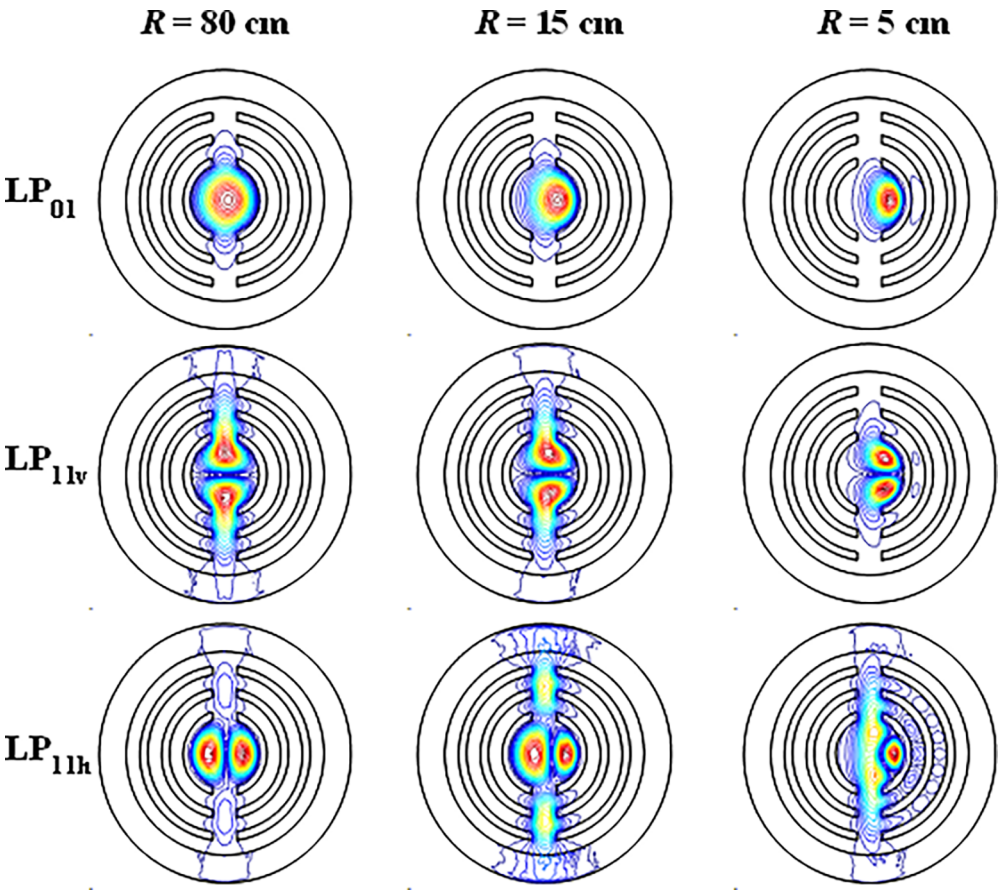

Fig 12. Contour line graphs of the mode field distribution of LP_{01}, LP_{11v} and LP_{11h} mode of the leaky-MTF with R = 80 cm, 15 cm and 5 cm.

https://doi.org/10.1371/journal.pone.0203047.g012

the mode distribution concentrates to the right side and the leakage loss reduced. So *Loss (LP_{01})* decreases with reducing bending radius. It is the same for *Loss (LP_{11v})*. When R = 80 cm, LP_{11v} mode suffers large loss because the mode leaks from gaps. LP_{11v} mode's loss leaks a lot to the fiber cladding. When R decreases, at R = 15 cm, the leaked energy decreases. When R = 5 cm, the mode moves to the right and less energy leaks to the cladding.

Since the gap breaks the circular symmetry of MTF, the discussion of bending direction is necessary. Fig 13 illustrates leakage losses of LP_{01} LP_{11v} and LP_{11h} modes and mode area of FM at varying bending orientation. When the bending orientation increases from 0 to 45˚, *Loss (LP_{01})* and *Loss (LP_{11v})* increases. However, *Loss (LP_{11h})* decreases and reaches a minimum value at Φ = 35˚. The inset picture shows the field distribution of LP_{11h} mode at Φ = 35˚. The mode area of FM has an obvious increase when bending orientation ranges from 0 to 30˚. Moreover, the effect of Φ on the performance is analyzed further, because Φ is a critical parameter when the fiber is bended.

Joint effects of gap and bending orientation

The joint effects of bending orientation and gap width are shown in Fig 14. The loss of FM, lowest-HOM, LR and mode area are plotted in Fig 14A–14D, respectively. Fig 14(A) shows that, the loss of FM increases with the increase of bending orientation and gap width. Fig 14

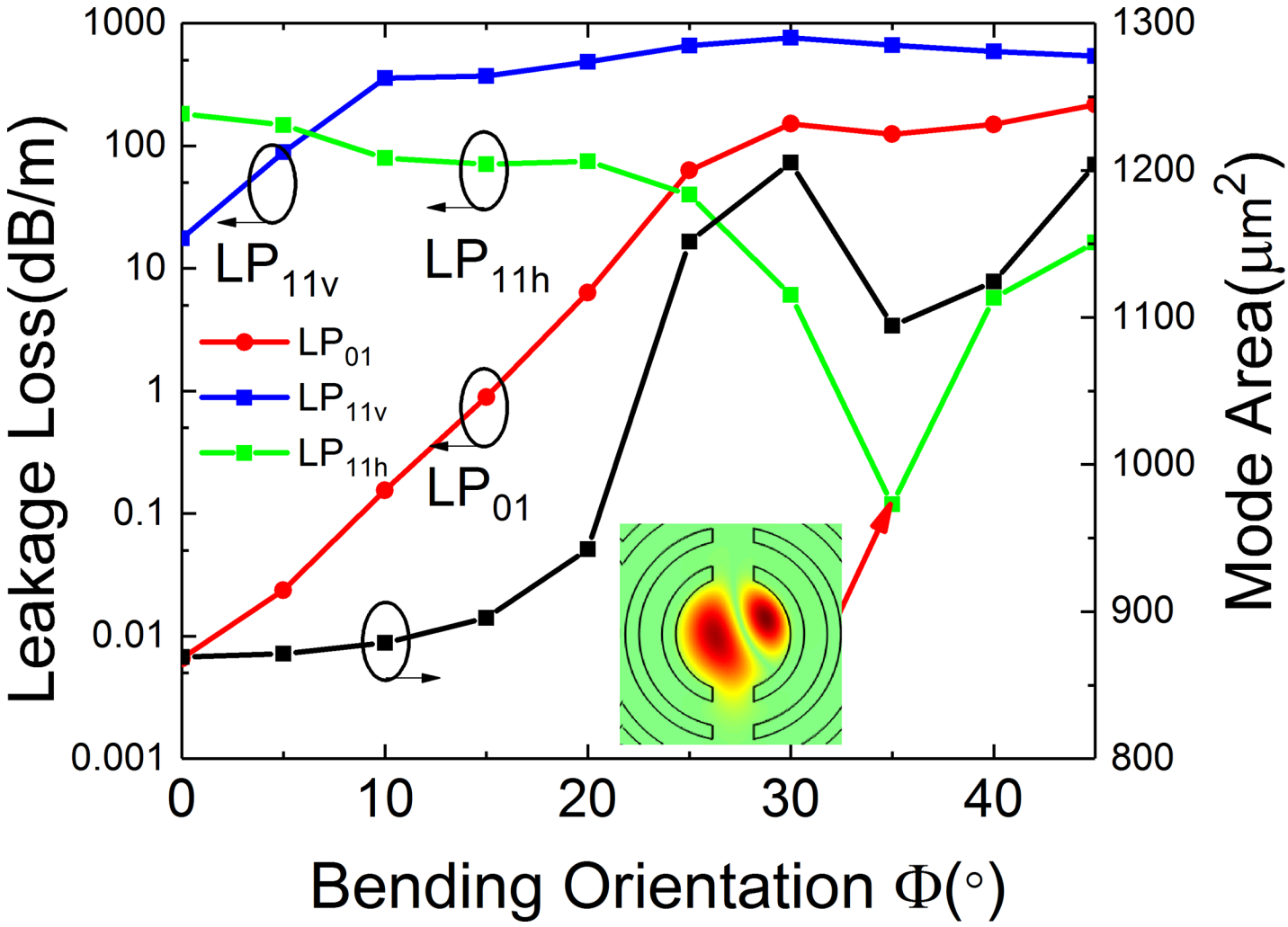

Fig 13. Simulated losses of the FM and HOMs and mode area of FM of the leaky-MTF with a = 25 μm, t_{gap} = 18 μm, t = 6 μm, d = 10 μm, R = 15 cm and Δn = 0.007 for different bending orientation.

https://doi.org/10.1371/journal.pone.0203047.g013

(B) shows that, the lowest loss of HOMs increases with the increases of gap width. However, the lowest loss of HOMs increases when Φ ranges from 0 to 10˚. Then it decreases when Φ ranges from 10˚ to 30˚. It is because that, $Loss(LP_{11v})$ is smaller than $Loss(LP_{11h})$ with small bending orientation, while larger than $Loss(LP_{11h})$ with large bending orientation. The lowest loss of HOMs increases and then decreases with bending orientation enlarges. It is obvious from Fig 13(C) that, the LR is large when the bending orientation is small. The LR increases with the increases of gap width. However, it has a maximum value with a proper gap width (at t_{gap} = 18 μm). The characteristic is corresponding with the conclusion obtained from Fig 4. It can be seen that, when Φ is less than 10˚ and t_{gap} ranges from 15 to 20 μm, the LR is larger than 100, which indicates that it conforms SM operation conditions. The A_{eff} increases when t_{gap} and Φ increase. It is because the leakage of FM is easier with greater bending and larger gap.

Effects of one parameter changes

The discussion above of parameter (t) is assumed the thickness of low RI trenches change synchronously. So does the thickness of high RI rings (d) and the gap width (t_{gap}). Next, we discuss

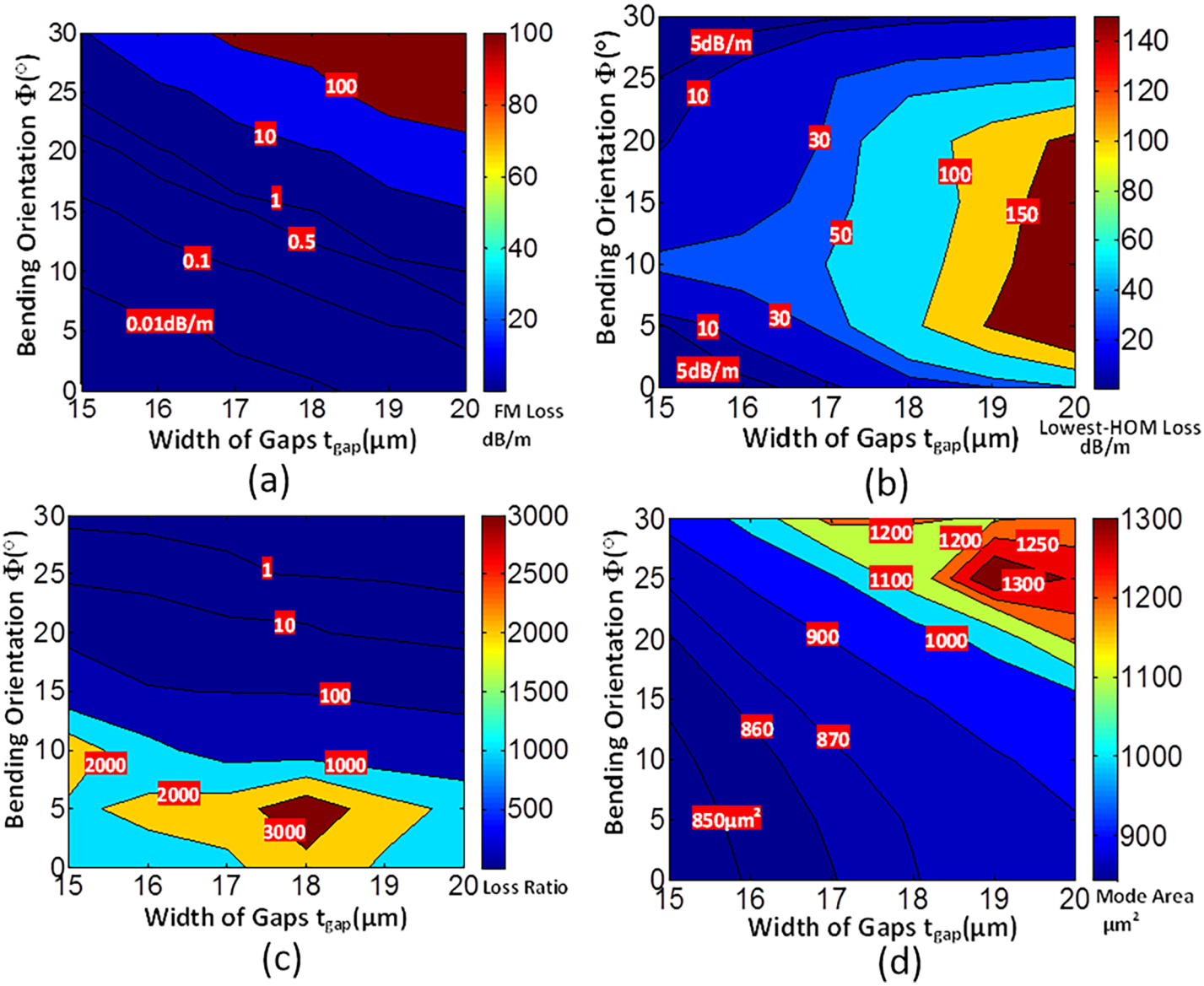

Fig 14. Joint effects of bending orientation (Φ) and gap width (t_{gap}) on (a) loss of FM, (b) loss of lowest-HOMs, (c) LR and (d) mode area with a = 25 μm, t = 6 μm, d = 10 μm, R = 15 cm and Δn = 0.007.

https://doi.org/10.1371/journal.pone.0203047.g014

the cases when there is only one parameter changing. Assume the fiber parameters are: a = 25 μm, t = 6 μm, d = 10 μm, t_{gap} = 18 μm, Δn = 0.007 and R = 15 cm. Fig 15A–15C show the losses of LP_{01}, LP_{11v} and LP_{11h} modes and the mode of FM with different low RI trench thickness t_1, t_2 and t_3, respectively. It can be seen that, t_1, t_2 and t_3 has a small influence on the losses of LP_{01}, LP_{11v} and LP_{11h} modes. t_1 has a big influence on A_{eff} of FM. However, t_2 and t_3 has a small influence on A_{eff}. The effect of one low RI trench is weak.

Fig 16(A) abd 16(B) show the losses of LP_{01}, LP_{11v} and LP_{11h} modes and the mode are of FM with different high RI ring thickness d_1 and d_2, respectively. d_1 and d_2 have small influence on the losses of LP_{01}, LP_{11v} and LP_{11h} modes and A_{eff} of FM. The effect of one high RI ring thickness is weak.

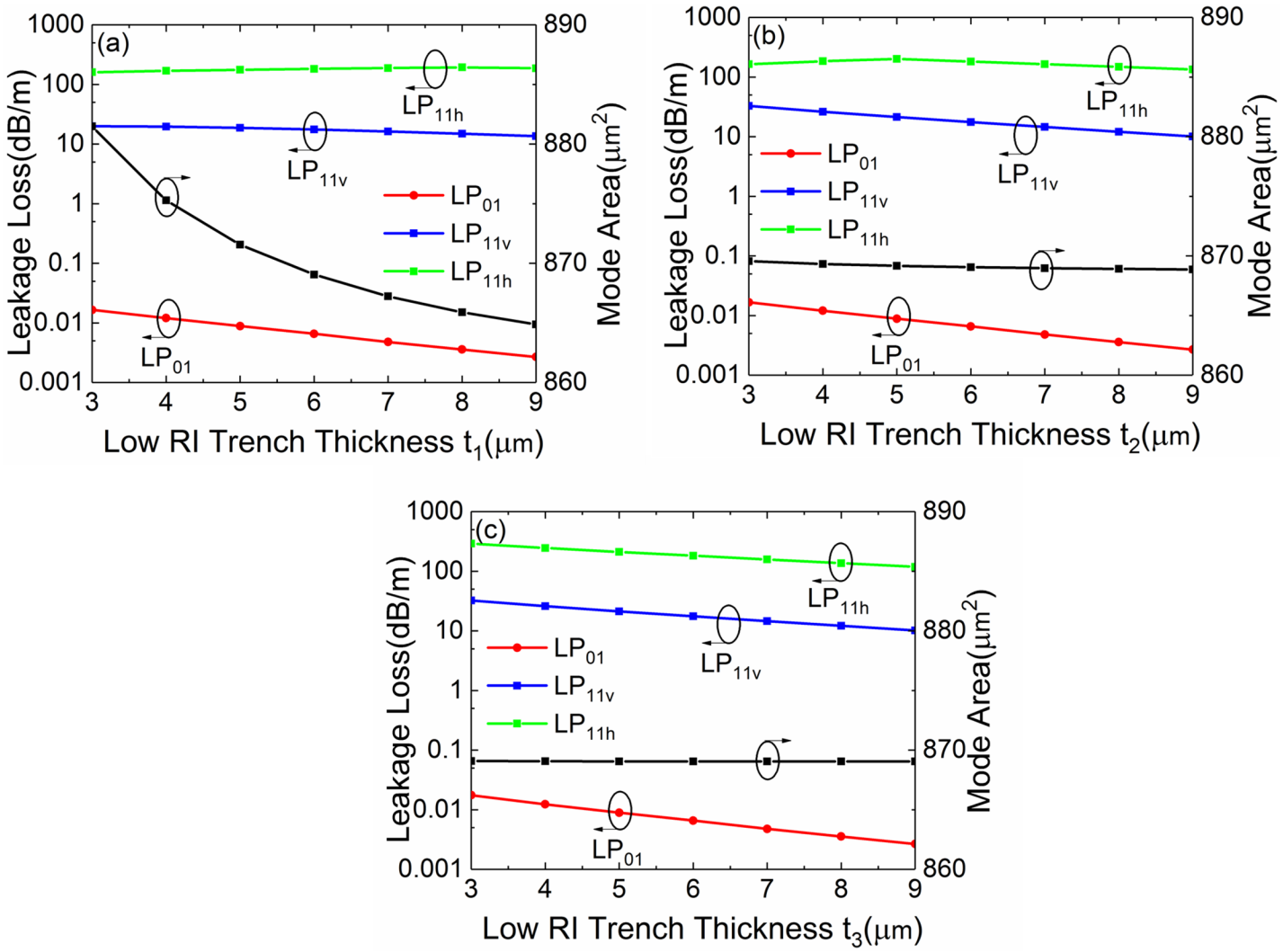

Fig 15. (a-c) Simulated losses of the FM and HOMs and mode area of FM of the leaky-MTF with a = 25 μm, t_{gap} = 18 μm, t = 6 μm, d = 10 μm, R = 15 cm and Δn = 0.007 for different t_1, t_2 and t_3, respectively.

https://doi.org/10.1371/journal.pone.0203047.g015

Fig 17A–17C show the losses of LP_{01}, LP_{11v} and LP_{11h} modes and the mode are of FM with different gap width t_{g1}, t_{g2} and t_{g3}, respectively. t_{g1}, t_{g2} and t_{g3} have small influence on the losses of LP_{01}, LP_{11v} and LP_{11h} modes and A_{eff} of FM. t_{g1} has a big influence on A_{eff} of FM. However, t_{g2} and t_{g3} have small influence on A_{eff}. The effect of one gap width is weak.

Numerical analysis results demonstrate that when there is only one parameter changing, the fiber confirms to single mode operation.

Conclusion

A novel design of multi-trench fiber (MTF) with gaps is proposed and investigated in this paper. This fiber shows more excellent single-mode (SM) operation than standard MTF. The fiber can achieve mode area of 840 μm^2 with high loss ratio (>300) under a tight bending radius of 15 cm. It has a special character that leakage loss decreases with the decreases of bending radius. The fiber can achieve better SM operation with smaller bending radius. The fiber performance is resistant to one parameter variation that, it allows small errors during

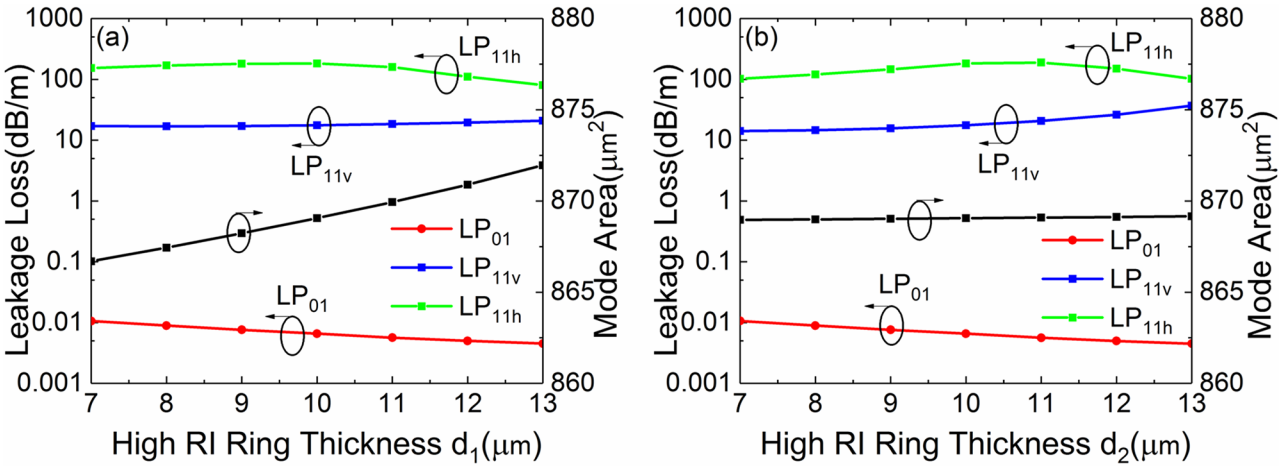

Fig 16. (a-b) Simulated losses of the FM and HOMs and mode area of FM of the leaky-MTF with a = 25 μm, t_{gap} = 18 μm, t = 6 μm, d = 10 μm, R = 15 cm and Δn = 0.007 for different d_1 and d_2, respectively.

https://doi.org/10.1371/journal.pone.0203047.g016

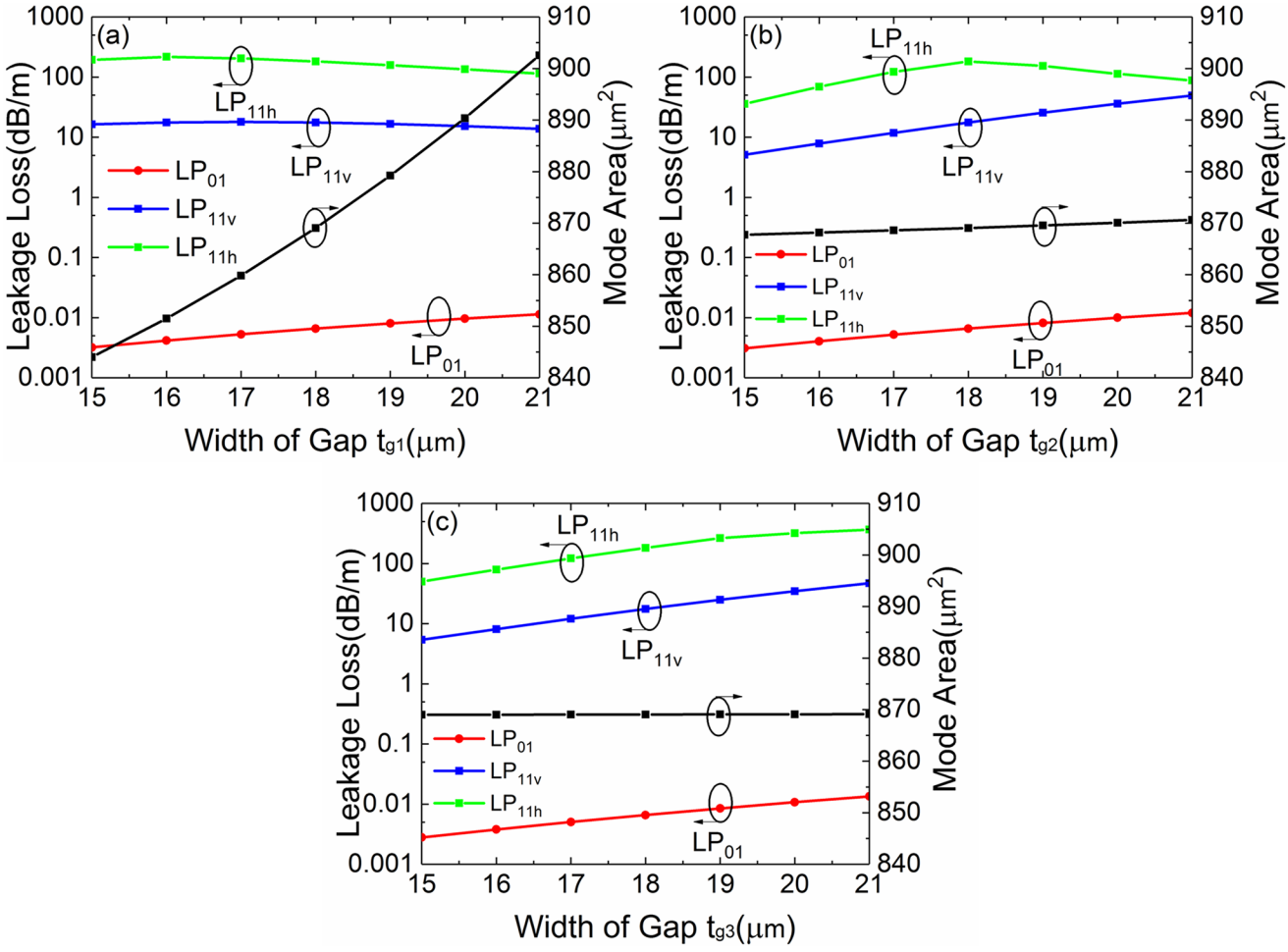

Fig 17. (a-c) Simulated losses of the FM and HOMs and mode area of FM of the leaky-MTF with a = 25 μm, t_{gap} = 18 μm, t = 6 μm, d = 10 μm, R = 15 cm and Δn = 0.007 for different t_{g1}, t_{g2} and t_{g3}, respectively.

https://doi.org/10.1371/journal.pone.0203047.g017

practical fabrication. This design shows the potential of mode field scaling and makes a contribution to compact high power fiber lasers.

Our present work is based on theoretical analysis. We are currently fabricating this fiber and the actual performance will be tested in the near future.

Author Contributions

Conceptualization: Shaoshuo Ma.

Data curation: Xiaodong Wen.

Formal analysis: Jing Li.

Funding acquisition: Li Pei.

Investigation: Xueqing He.

Methodology: Tigang Ning.

Project administration: Li Pei.

Software: Xueqing He.

Supervision: Tigang Ning.

Validation: Jingjing Zheng.

Writing – original draft: Shaoshuo Ma.

Writing – review & editing: Shaoshuo Ma, Tigang Ning, Xueqing He.

References

1. Nilsson J, Payne DN (2011) Physics. High-power fiber lasers. Science 332: 921–922. https://doi.org/10.1126/science.1194863 PMID: 21596979
2. Richardson D, Nilsson J, Clarkson W (2010) High power fiber lasers: current status and future perspectives [Invited]. JOSA B 27: B63–B92.
3. Zervas MN, Codemard CA (2014) High power fiber lasers: a review. Selected Topics in Quantum Electronics, IEEE Journal of 20: 219–241.
4. Eidam T, Wirth C, Jauregui C, Stutzki F, Jansen F, et al. (2011) Experimental observations of the threshold-like onset of mode instabilities in high power fiber amplifiers. Optics Express 19: 13218. https://doi.org/10.1364/OE.19.013218 PMID: 21747477
5. Smith AV, Smith JJ (2011) Mode instability in high power fiber amplifiers. Optics express 19: 10180–10192. https://doi.org/10.1364/OE.19.010180 PMID: 21643276
6. Machewirth D, Khitrov V, Manyam U, Tankala K, Carter A, et al. (2004) Large-mode-area double-clad fibers for pulsed and CW lasers and amplifiers. Proceedings of SPIE—The International Society for Optical Engineering 5335: 140–150.
7. Li M-J, Chen X, Liu A, Gray S, Wang J, et al. (2009) Limit of effective area for single-mode operation in step-index large mode area laser fibers. Journal of Lightwave Technology 27: 3010–3016.
8. Ma X, Zhu C, Hu IN, Kaplan A, Galvanauskas A (2014) Single-mode chirally-coupled-core fibers with larger than 50 μm diameter cores. Optics Express 22: 9206–9219. https://doi.org/10.1364/OE.22.009206 PMID: 24787810
9. Limpert J, Liem A, Reich M, Schreiber T, Nolte S, et al. (2004) Low-nonlinearity single-transverse-mode ytterbium-doped photonic crystal fiber amplifier. Optics Express 12: 1313. PMID: 19474951
10. Rastogi V, Chiang KS (2004) Analysis of segmented-cladding fiber by the radial-effective-index method. JOSA B 21: 258–265.
11. Ma S, Ning T, Li J, Pei L, Zhang C, et al. (2016) Detailed study of bending effects in large mode area segmented cladding fibers. Applied Optics 55: 9954. https://doi.org/10.1364/AO.55.009954 PMID: 27958396
12. Kim G, Richardson M, Bass M, Mccomb T, Sudesh V, et al. (2010) Diode Side Pumping of a Gain Guided, Index Anti-Guided Large Mode Area Neodymium Fiber Laser. Advanced Solid.

13. Wang L, He D, Yu C, Feng S, Hu L, et al. (2016) Very Large-Mode-Area, Symmetry-Reduced, Neodymium-Doped Silicate Glass All-Solid Large-Pitch Fiber. IEEE Journal of Selected Topics in Quantum Electronics 22: 108–112.
14. Molardi C, Poli F, Rosa L, Selleri S, Cucinotta A (2017) Mode discrimination criterion for effective differential amplification in Yb-doped fiber design for high power operation. Optics Express 25: 29013.
15. Kumar A, Dussardier B, Monnom G, Rastogi V (2011) Large-mode-area leaky optical fiber fabricated by MCVD. Applied Optics 50: 3118–3122. https://doi.org/10.1364/AO.50.003118 PMID: 21743510
16. Kumar A, Rastogi V (2007) Design and analysis of a multilayer cladding large-mode-area optical fibre. Journal of Optics A: Pure and Applied Optics 10: 015303.
17. Kumar A, Rastogi V (2011) Design and analysis of dual-shape-core large-mode-area optical fiber. Applied Optics 50: E119–E124.
18. Jain D, Baskiotis C, May-Smith TC, Kim J, Sahu JK (2014) Large mode area multi-trench fiber with delocalization of higher order modes. Selected Topics in Quantum Electronics, IEEE Journal of 20: 242–250.
19. Jain D, Baskiotis C, Sahu JK (2013) Bending performance of large mode area multi-trench fibers. Optics express 21: 26663–26670. https://doi.org/10.1364/OE.21.026663 PMID: 24216887
20. Jain D, Baskiotis C, Sahu JK (2013) Mode area scaling with multi-trench rod-type fibers. Optics express 21: 1448–1455. https://doi.org/10.1364/OE.21.001448 PMID: 23389126
21. Sun J, Qi Y, Kang Z, Ma L, Jian S (2015) A Modified Bend-Resistant Multitrench Fiber With Two Gaps. Lightwave Technology, Journal of 33: 4908–4914.
22. Sun J, Kang Z, Ji J, Yoo S, Nilsson J, et al. (2015) Multi-trench fiber with four gaps for improved bend performance. Applied optics 54: 8271–8274. https://doi.org/10.1364/AO.54.008271 PMID: 26479595
23. Tsuchida Y, Saitoh K, Koshiba M (2005) Design and characterization of single-mode holey fibers with low bending losses. Optics Express 13: 4770–4779. PMID: 19495395
24. Nagano K, Kawakami S, Nishida S (1978) Change of the refractive index in an optical fiber due to external forces. Applied optics 17: 2080–2085. https://doi.org/10.1364/AO.17.002080 PMID: 20203728
25. Petermann K (1983) Constraints for Fundamental-Mode Spot Size for Broadband Dispersion-Compensated Single-Mode Fibers. Electronics Letters 19: 712–714.
26. Saitoh K, Koshiba M (2003) Leakage loss and group velocity dispersion in air-core photonic bandgap fibers. Optics Express 11: 3100. PMID: 19471432
27. Wang X, Lou S, Lu W, Sheng X, Zhao T, et al. (2016) Bend Resistant Large Mode Area Fiber With Multi-Trench in the Core. Selected Topics in Quantum Electronics, IEEE Journal of 22: 1–8.